Materials Research Bulletin 48 (2013) 2040–2043

Contents lists available at SciVerse ScienceDirect

Materials Research Bulletin

journal homepage: www.elsevier.com/locate/matresbu

Preparation, crystal structure and properties of $HoBaCo_{2-x}Fe_xO_{5+\delta}$

L. Ya. Gavrilova, N.E. Volkova, T.V. Aksenova, V.A. Cherepanov *

Ural Federal University, Yekaterinburg, Russia

ARTICLE INFO

Article history:
Received 30 August 2012
Received in revised form 29 January 2013
Accepted 11 February 2013
Available online 28 February 2013

Keywords:
A. Inorganic compounds
B. Chemical synthesis
C. Thermogravimetric analysis (TGA)
D. Crystal structure

ABSTRACT

A series of samples of overall composition $HoBaCo_{2-x}Fe_xO_{5+\delta}$ with $0.0 \le x \le 0.8$ were prepared by glycerin nitrate technique in air and in pure oxygen. Irrespective of atmosphere used the homogeneity range of single phase iron substituted holmium barium cobaltate was proved to exist within the range $0.0 \le x \le 0.4$. All samples prepared in air and samples within the compositional range $0.2 \le x \le 0.4$ obtained in oxygen possess tetragonal $a_p \times a_p \times 2a_p$ (sp. gr. P4/*mmm*) structure. $HoBaCo_2O_{5+\delta}$ and $HoBaCo_{1.9}Fe_{0.1}O_{5+\delta}$ synthesized in oxygen crystallized in orthorhombic $a_p \times 2a_p \times 2a_p$ (sp. gr. P*mmm*) structure. The structural parameters were refined by the Rietveld analysis. It was shown that parameter *a* remains practically constant while parameter *c* gradually increases with the increase of iron content. The changes of oxygen content in $HoBaCo_{2-x}Fe_xO_{5+\delta}$ ($x = 0$, 0.2, 0.4) were measured by TGA within the temperature range 25–1100 °C in air. The absolute value of oxygen content was determined by the reduction of the samples in hydrogen flow. The influence of oxygen and iron content on the crystal structure has been discussed. The chemical stability of $HoBaCo_{2-x}Fe_xO_{5+\delta}$ in contact with the solid electrolyte materials $Ce_{0.8}Sm_{0.2}O_2$ and $Zr_{0.85}Y_{0.15}O_2$ was examined.

1. Introduction

Layered perovskite-type phases $LnBaCo_2O_{5+\delta}$ (Ln = Pr–Ho, Y) attract intent attention of investigators as promising materials for different electrochemical applications, such as electrodes for the high temperature and intermediate temperature fuel cells and oxygen-conducting membranes [1–5].

The crystal structure and various physicochemical properties of undoped rare earth barium cobaltates $LnBaCo_2O_{5+\delta}$ (Ln = Pr–Ho) were intensively studied during the last decade [6–14]. The unit cell of the double perovskite $LnBaCo_2O_{5+\delta}$ in contrast to the ordinary one ABO_3 has doubled along the *c*-axis due to the ordered location of Ln and Ba cations [6,7]. Depending on oxygen content two types of Co coordination can appear: either square pyramid CoO_5 or octahedron CoO_6. When oxygen content in the oxide became equal to 5.5 an alternation of pyramids and octahedrons along the *b*-axis takes place, which is equivalent to ordering of oxygen vacancies and leads to the doubling of *b* parameter of the unit cell [6]. Thus variations of synthesis procedure or annealing conditions (temperature and oxygen partial pressure) of the double perovskites $LnBaCo_2O_{5+\delta}$ can result in the formation of either tetragonal P4/*mmm* ($a_p \times a_p \times 2a_p$) or orthorhombic P*mmm* ($a_p \times 2a_p \times 2a_p$) structure, where a_p: is the unit cell parameter of ideal perovskite.

General disadvantage of cobaltates while using as the cathodes for the solid oxide fuel cells is their high chemical activity toward the materials of solid electrolytes. A well known approach that is often used in order to increase the stability of materials is doping. One can expect that iron substitution $LnBaCo_{2-x}Fe_xO_{5+\delta}$ (Ln = Pr–Ho) will increase chemical stability of rare earth barium cobaltates [14–16]. However the information about the formation and properties of Fe-containing solid solution based on the $HoBaCo_2O_{5+\delta}$ is absent.

Therefore the aims of the present work are: (i) synthesis of the $HoBaCo_{2-x}Fe_xO_{5+\delta}$ solid solutions and determination of their homogeneity range; (ii) determination of crystal structure of the single phase solid solutions; (iii) determination of oxygen content as a function of temperature and (iv) evaluation of chemical stability of substituted samples in respect to the $Ce_{0.8}Sm_{0.2}O_2$ and $Zr_{0.85}Y_{0.15}O_2$, often used as solid electrolytes materials in the fuel cells.

2. Experimental

Synthesis of the samples for investigation was performed using glycerin nitrate technology. Holmium oxide Ho_2O_3 with the purity not less than 99.99%, barium carbonate $BaCO_3$ (special purity

* Corresponding author at: Department of Chemistry, Ural Federal University, Lenin av., 51, Yekaterinburg 620000, Russia. Tel.: +7 343 261 74 11; fax: +7 343 261 74 11.
E-mail addresses: Vladimir.cherepanov@usu.ru, vl_cherepanov@mail.ru (V.A. Cherepanov).

0025-5408/$ – see front matter © 2013 Elsevier Ltd. All rights reserved.
http://dx.doi.org/10.1016/j.materresbull.2013.02.027

grade), metallic cobalt and iron oxalate $FeC_2O_4 \times 2H_2O$ (pure for analysis grade), nitric acid and glycerin both pure for analysis grade were used as starting materials. Metallic cobalt was obtained by the reduction of Co_3O_4 (pure for analysis grade) in the hydrogen flow at 500–600 °C.

According to the glycerin–nitrate technique required amounts of starting materials were dissolved in the 4.5 M nitric acid while heating, then glycerin was added in amount equivalent to a complete reduction of nitrate groups. Obtained solution was dried to a viscous gel that further transformed to a brown powder. Solid residual was heated in steps within the temperature range 500–900 °C. After that obtained powders were pressed into pellets and finally annealed during 48 h at 1100 °C in air and in the flow of pure oxygen with intermediate grindings with following slow cooling to room temperature at the rate of about 100°/h.

The samples of solid electrolyte materials $Ce_{0.8}Sm_{0.2}O_2$ and $Zr_{0.85}Y_{0.15}O_2$ were obtained by glycerin nitrate technique and co-precipitation method respectively. The former was prepared using the procedure similar to described above using $Ce(CO_3)_2 \times 2H_2O$ and Sm_2O_3 as starting materials. In order to prepare $Zr_{0.85}Y_{0.15}O_2$ required amounts of $Zr(OH)_2CO_3 \times H_2O$ и Y_2O_3 were dissolved in nitric acid while heating, then aqueous solution of NH_4OH was added as precipitating agent. Resulting amorphous precipitate was thoroughly washed by water, dried at 100 °C during 6 h and finally annealed at 700 °C during 10 h.

Phase identification was made by XRD analysis (DRON-6 diffractometer, Cu-Kα radiation, angle range 2θ = 10–100°, step 0.02°, 10 s/step). The unit cell parameters were calculated using "CelRef 4.0" program and refined using full profile Rietveld analysis [17,18].

The changes of oxygen content in $HoBaCo_{2-x}Fe_xO_{5+\delta}$ were measured by thermogravimetric analysis (TGA) within the temperature range $25 \leq T,^{\circ}C \leq 1100$ in air using simultaneous thermal analyzer STA 409 PC Luxx, Netzsch. The measurements were performed with the cooling/heating rate equal to 0.5°/min. The absolute oxygen content in the samples was determined using a direct reduction of the samples in the TG cell by hydrogen (10% H_2–90% Ar) assuming Ho_2O_3, BaO and metallic Co and Fe as final products.

Chemical stability of the $HoBaCo_{2-x}Fe_xO_{5+\delta}$ relative to the electrolyte materials $Ce_{0.8}Sm_{0.2}O_2$ and $Zr_{0.85}Y_{0.15}O_2$ has been checked within the temperature range 900–1100°C, by means of annealing of the corresponding mixtures with 1:1 weight ratio during 24 h in air with following XRD analysis.

3. Results and discussion

In order to determine the homogeneity range of iron substituted holmium barium cobaltate a series of samples with overall composition $HoBaCo_{2-x}Fe_xO_{5+\delta}$ within $0.0 \leq x \leq 0.8$ in step $x = 0.1$ was prepared in air ($P_{O_2} = 0.21$ atm) and in pure oxygen ($P_{O_2} = 1.0$ atm). According to the results of XRD analysis single phase samples were formed within the range $0.0 \leq x \leq 0.4$ irrespective of atmosphere used.

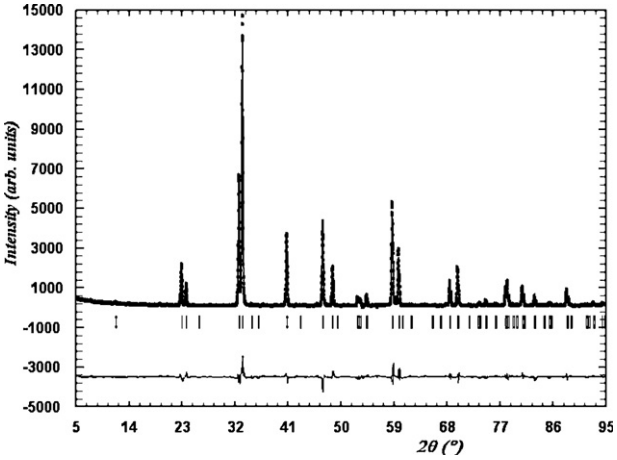

Fig. 1. Rietveld refinement profile of $HoBaCo_2O_{5+\delta}$. The circles and upper continuous plot correspond to the experimental data points and calculated profile, respectively. The lower line is the difference plot.

X-ray diffraction pattern obtained for the undoped $HoBaCo_2O_{5+\delta}$, prepared in air, was indexed in tetragonal structure ($a_p \times a_p \times 2a_p$), sp. gr. *P4/mmm*, with the unit cell parameters $a = b = 3.876$ Å, $c = 7.490$ Å, that is in a good agreement with previously reported [6–8,19]. Fig. 1 illustrates X-ray diffraction pattern for $HoBaCo_2O_{5+\delta}$ refined by the Rietveld analysis. All iron substituted single phase holmium barium cobaltates $HoBaCo_{2-x}Fe_xO_{5+\delta}$ ($0.0 < x \leq 0.4$) obtained in air possess tetragonal $a_p \times a_p \times 2a_p$ (sp. gr. *P4/mmm*) structure similar to undoped oxide. The structural parameters for all single phase solid solutions $HoBaCo_{2-x}Fe_xO_{5+\delta}$ were also refined by the Rietveld method (Table 1). Fig. 2 shows that parameter *a* remains practically constant while parameter *c* gradually increases with the increase of iron content. Such behavior can be explained size factor since the ionic radius of iron is larger than ionic radius of cobalt ($r_{Fe^{3+}} = 0.785$ Å; $r_{Co^{3+}} = 0.75$ Å, both for C.N. = 6) [20]. However the difference in the 3d cation sizes should influence both *a* and *c* parameters. Another probable reason of such behavior linked with the peculiarity of oxygen vacancies location in the structure of double perovskites $LnBaCo_2O_{5+\delta}$. It is well recognized that oxygen vacancies are not randomly distributed in the lattice, but located in the Ln–O planes [6]. As it will be shown below, the substitution of Co ions by Fe leads to the increase of oxygen content and as a result has move apart the layers along *c*-axis while the value of *a* parameter remains practically unchanged.

Fig. 3 represents the results of XRD measurements of slowly cooled single phase $HoBaCo_{2-x}Fe_xO_{5+\delta}$ ($0.0 \leq x \leq 0.4$) prepared in pure oxygen. The splitting of peaks at the angles 22.7° and 46.6° on X-ray diffraction patterns of $HoBaCo_2O_{5+\delta}$ and $HoBaCo_{1.9}Fe_{0.1}O_{5+\delta}$

Table 1
The structural parameters and *R*-factors refined by the Rietveld method of the single phase $HoBaCo_{2-x}Fe_xO_{5+\delta}$ ($0.0 \leq x \leq 0.4$) solid solutions prepared in air.

P4/mmm space group, Ho (0.5, 0.5, 0), Ba (0.5, 0.5, 0.5), Co/Fe (0, 0, *z*), O1 (0, 0, 0), O2 (0, 0, 0.5), O3 (0, 0.5, *z*)					
x	0	0.1	0.2	0.3	0.4
a, Å	3.876(1)	3.874(1)	3.875(1)	3.877(1)	3.875(1)
c, Å	7.490(1)	7.490(1)	7.496(1)	7.507(1)	7.528(1)
V, Å^3	112.59 (2)	112.44(2)	112.56(2)	112.85 (2)	113.06(2)
z (Co/Fe)	0.242 (2)	0.243(2)	0.243(1)	0.243(2)	0.244(2)
z (O3)	0.201(2)	0.198(2)	0.199**(3)**	0.194(2)	0.199(2)
R_{Br}	6.76%	6.01%	7.71%	7.66%	5.43%
R_f	6.93%	6.06%	7.39%	7.26%	6.58%
R_p	14.7%	10.2%	12.8%	11.0%	11.7%

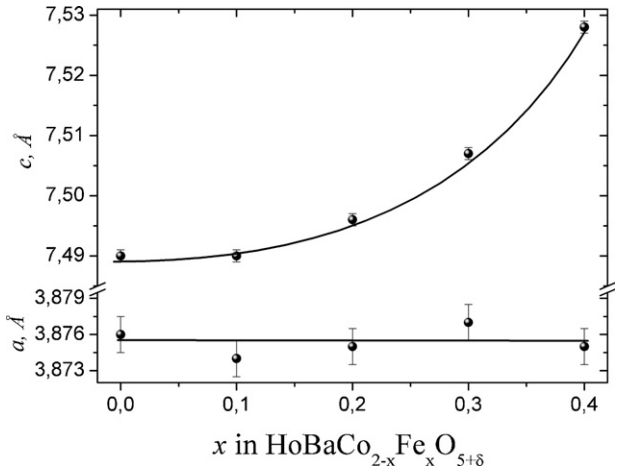

Fig. 2. The unit cell parameters for the $HoBaCo_{2-x}Fe_xO_{5+\delta}$ versus composition of the solid solution.

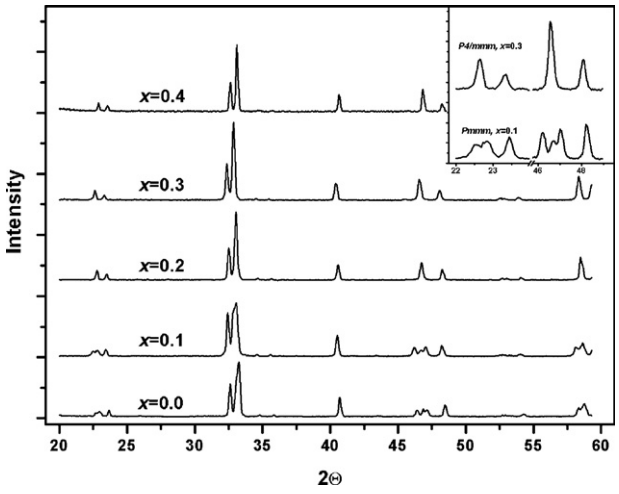

Fig. 3. X-ray diffraction profiles of the $HoBaCo_{2-x}Fe_xO_{5+\delta}$, prepared in oxygen. The inserts show an absence (upper line) and appearance (lower line) of splitting of the peaks at ~22.7° and 46.6°.

(see insert in the Fig. 3) proved the formation of orthorhombic structure ($a_p \times 2a_p \times 2a_p$) with the sp. gr. *Pmmm*. The samples with $x = 0.2$, 0.3 and 0.4 obtained in pure oxygen crystallized in tetragonal cell $a_p \times a_p \times 2a_p$ (sp. gr. *P4/mmm*) similar to those prepared in air (Fig. 3). The structural parameters refined by Rietveld analysis for the $HoBaCo_{2-x}Fe_xO_{5+\delta}$ synthesized in oxygen are listed in Table 2.

The results of TGA measurements for the $HoBaCo_{2-x}Fe_xO_{5+\delta}$ with $x = 0$, 0.2 and 0.4 versus temperature in air are shown in Fig. 4. It can be seen that oxygen exchange between the solid and gaseous phases has started at about 300°C. An introduction of iron into the holmium barium cobaltate increases the oxygen content. These can be explained by the fact that iron as more electropositive cation in comparison to cobalt ($\chi_{Fe} = 1.64$; $\chi_{Co} = 1.7$ in the Allred and Rochow scale [21]), acts partially or completely as an electron donor impurity $Fe^{\bullet}_{Co}$ and therefore hampers oxygen release process. Similar behavior was observed in the ordinary perovskite systems $Ln_{1-x}Me_xCo_{2-y}Fe_yO_{3-\delta}$ (Me = alkali earth metals) [22,23].

Taking into account that the value of oxygen content in the undoped $HoBaCo_2O_{5+\delta}$ at room temperature in the air is equal to 5.38 one can expect that it has to increase toward 5.5 in pure oxygen. For example, the value of oxygen content in the $HoBaCo_2O_{5+\delta}$, prepared in oxygen, was reported to be equal to 5.5 [6] and 5.511 [10]. As it was reported earlier [6] the orthorhombic structure ($a_p \times 2a_p \times 2a_p$) with *b* parameter doubling takes place when oxygen index tends to a value 5.5, however the range of oxygen content that corresponds to orthorhombic structure can vary with the rare earth nature [7]. The situation became more complicated in the Fe-doped

Table 2
The structural parameters and **R**-factors refined by the Rietveld method of the single phase $HoBaCo_{2-x}Fe_xO_{5+\delta}$ ($0.0 \le x \le 0.4$) solid solutions prepared in oxygen.

	Orthorhombic cell, Pmmm space group, Ho (0.5, *y*, 0.5), Ba (0.5, *y*, 0), Co/Fe1 (0, 0.5, *z*), Co/Fe2 (0, 0, *z*), O1 (0, 0, 0), O2 (0, 0.5, 0), O3 (0, 0.5, 0.5), O4 (0, 0, 0.5), O5 (0.5, 0, *z*), O6 (0.5, 0.5, *z*), O7 (0, *y*, *z*)		
x	0	0.1	
a, Å	3.855(1)	3.850(1)	
b, Å	7.806(1)	7.815(1)	
c, Å	7.503(1)	7.513(1)	
V, Å^3	225.80(2)	226.04(2)	
y (Ho)	0.244(2)	0.248(2)	
y (Ba)	0.266(1)	0.266(1)	
z (Co/Fe)1	0.249(1)	0.251(1)	
z (Co/Fe)2	0.247(2)	0.247(2)	
z (O5)	0.189(3)	0.205(3)	
z (O6)	0.211(3)	0.206(3)	
y (O7)	0.203(2)	0.212(2)	
z (O7)	0.228(1)	0.206(1)	
R_{Br}	9.7%	5.8%	
R_f	10.9%	5.9%	
R_p	11.0%	11.2%	
	Tetragonal cell, P4/mmm space group, Ho (0.5, 0.5, 0), Ba (0.5, 0.5, 0.5), Co/Fe (0, 0, *z*), O1 (0, 0, 0), O2 (0, 0, 0.5), O3 (0, 0.5, *z*)		
x	0.2	0.3	0.4
a, Å	3.872 (1)	3.874 (1)	3.872 (1)
c, Å	7.514 (1)	7.525 (1)	7.528 (1)
V, Å^3	112.67 (2)	112.92 (2)	112.85 (2)
z (Co/Fe)	0.250(2)	0.249(2)	0.242(2)
z (O3)	0.204(2)	0.204(2)	0.197(2)
R_{Br}	6.22%	6.68%	5.67%
R_f	5.37%	5.56%	7.86%
R_p	9.3%	8.3%	10.9%

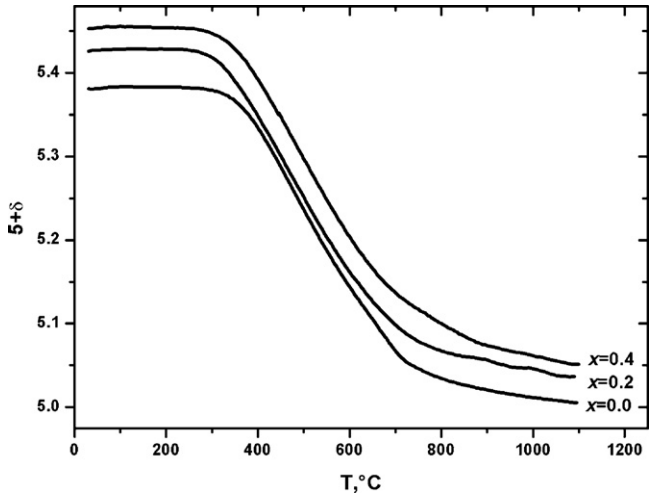

Fig. 4. Variations of oxygen content in $HoBaCo_{2-x}Fe_xO_{5+\delta}$ in air.

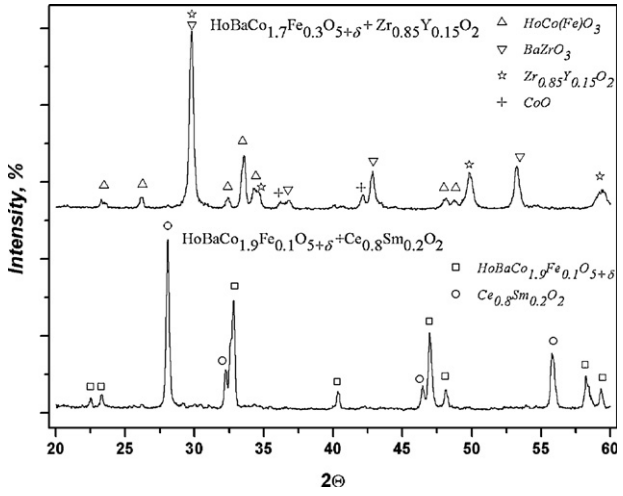

Fig. 5. XRD patterns of the $HoBaCo_{2-x}Fe_xO_{5+\delta}$ samples in contact with the $Zr_{0.85}Y_{0.15}O_2$ and $Ce_{0.8}Sm_{0.2}O_2$ fired at 900 °C.

samples. Since Fe ions act as electron donor impurity $Fe_{Co}^{\bullet}$ while cobalt electron acceptor centers $Co_{Co}^{'}$ the distribution of oxygen vacancies $V_O^{\bullet\bullet}$ will be influenced by 3d ions sublattice. One can expect that while Fe/Co ratio is far from 1/1, but large enough to become sensitive, a random distribution of $Fe_{Co}^{\bullet}$ ions will act as disordering agent for the oxygen vacancies $V_O^{\bullet\bullet}$. This could be the reason that $HoBaCo_{1.6}Fe_{0.4}O_{5.45}$ obtained in air has remained the tetragonal ($a_p \times a_p \times 2a_p$) structure. The samples with x = 0.2, 0.3 and 0.4 obtained in pure oxygen crystallized in the tetragonal cell $a_p \times a_p \times 2a_p$ due to the mentioned above reason and also because of increase of the oxygen content.

According to the results of XRD the samples $HoBaCo_{2-x}Fe_xO_{5+\delta}$ with $x \geq 0.5$ were multiphase. The samples with $x = 0.5$–0.8 in step 0.1 annealed in air and with $x = 0.5$ and 0.6 prepared in oxygen contained besides the saturated solid solution with approximate composition $HoBaCo_{1.6}Fe_{0.4}O_{5+\delta}$ two additional phases: $HoFeO_{3-\delta}$ and $BaCoO_{3-\delta}$, or solid solutions based on these phases. The samples with $x = 0.7$ and 0.8 fired in oxygen consisted of saturated $HoBaCo_{1.6}Fe_{0.4}O_{5+\delta}$, $HoFeO_{3-\delta}$ or solid solution based on it and additional unknown phase with the cubic structure.

Chemical compatibility of the $HoBaCo_{1.9}Fe_{0.1}O_{5+\delta}$ and $HoBaCo_{1.7}Fe_{0.3}O_{5+\delta}$ with the solid electrolyte materials has been checked in air within the temperature range 900–1100 °C. It was found that $HoBaCo_{2-x}Fe_xO_{5+\delta}$ interacts with the $Zr_{0.85}Y_{0.15}O_2$ even at 900 °C forming $BaZrO_3$, $HoCo_{1-x}Fe_xO_3$ and CoO as the products. Since barium zirconate reveals low conductivity $HoBaCo_{2-x}Fe_xO_{5+\delta}$ cannot be recommended as electrode materials in the contact with YSZ electrolyte.

In contrast $HoBaCo_{1.9}Fe_{0.1}O_{5+\delta}$ and $HoBaCo_{1.7}Fe_{0.3}O_{5+\delta}$ were chemically stable in contact with $Ce_{0.8}Sm_{0.2}O_2$ at 900°C and 1000°C. However anneals at 1100 °C show beginning of chemical interaction between $HoBaCo_{2-x}Fe_xO_{5+\delta}$ and $Ce_{0.8}Sm_{0.2}O_2$. Fig. 5 illustrates the results of XRD patterns of the $HoBaCo_{2-x}Fe_xO_{5+\delta}$ and electrolyte materials mixtures annealed at 900 °C as an example.

4. Conclusion

XRD analysis shows that homogeneity range of $HoBaCo_{2-x}Fe_xO_{5+\delta}$ solid solution has not exceeded the value x = 0.4 either in air or in pure oxygen, with accuracy in x value 0.1. Substitution of Co by Fe influences both the value of oxygen content and crystal structure of the $HoBaCo_{2-x}Fe_xO_{5+\delta}$. It was shown that $HoBaCo_{2-x}Fe_xO_{5+\delta}$ solid solutions are chemically stable in the contact with $Ce_{0.8}Sm_{0.2}O_2$ at 900 °C and 1000 °C, but interact with $Zr_{0.85}Y_{0.15}O_2$ even at 900 °C.

Acknowledgements

This work was financially supported in parts by the Russian Foundation for Basic Research (project no. 12-03-91663) and the Ministry for Education and Science of the Russian Federation within the Federal Target Program "Investigations and researchers on the priority directions of development for the scientific and technological complex of Russia in 2007–2013".

References

[1] J.-H. Kim, A. Manthiram, J. Electrochem. Soc. 155 (2008) 385–390.
[2] K. Zhang, L. Ge, R. Ran, et al. Acta Mater. 56 (2008) 4876–4889.
[3] A. Tarascon, S.J. Skinner, R.J. Chater, F. Hernandez-Ramirez, J.A. Kilner, J. Mater. Chem. 17 (2007) 3175–3181.
[4] C. Zhu, X. Liu, C. Yi, D. Yan, W. Su, J. Power Sources 185 (2008) 193–196.
[5] A. Tarancón, J. Peña-Martínez, D. Marrero-López, A. Morata, J.C. Ruiz-Morales, P. Núñez, Solid State Ionics 179 (2008) 2372–2378.
[6] A. Maignan, C. Martin, D. Pelloquin, N. Nguyen, B. Raveau, J. Solid State Chem. 142 (1999) 247–260.
[7] P.S. Anderson, C.A. Kirk, J. Knudsen, I.M. Reaney, A.R. West, J. Solid State Sci. 7 (2005) 1149–1156.
[8] L. Malavasi, Yu Diaz-Fernandez, C.-M. Mozzati, C. Ritter, Solid State Ionics 148 (2008) 87–90.
[9] K. Conder, E. Pomjakushina, A. Soldatov, E. Mitberg, Mater. Res. Bull. 40 (2005) 257–263.
[10] E-L. Rautama, M. Karppinen, J. Solid State Chem. 183 (2010) 1102–1107.
[11] C. Frontera, M. Respaud, J.L. García-Munõz, A. Llobet, A.E. Carrillo, A. Caneiro, J.M. Broto, Physica B 346/347 (2004) 246–249.
[12] J.-E. Jorgensen, L. Keller, Phys. Rev. B 77 (2008) 024427-1–024427-6.
[13] A.A. Taskin, A.N. Lavrov, Y. Ando, Prog, Solid State Chem. 35 (2007) 481–490.
[14] X. Zhang, H. Hao, O. He, X. Hu, Physica B 394 (2007) 118–121.
[15] D.D. Khalyavin, A.M. Balagurov, A.I. Beskrovnyi, I.O. Troyanchuk, A.P. Sazonov, E.V. Tsipis, V.V. Kharton, J. Solid State Chem. 177 (2004) 2068–2072.
[16] N. Thirumurugan, A. Bharathi, C.S. Sundar, J. Magn. Magn. Mater. 322 (2010) 152–157.
[17] V.K. Pecharsky, P.Y. Zavalij, Fundamentals of Powder Diffraction and Structural Characterization of Materials, 2nd ed., Springer, New York, 2005.
[18] R.E. Dinnebier, S.J.L. Billinge, Powder Diffraction. Theory and Practice, RSC Publishing, Cambridge, 2008.
[19] E. Suard, F. Fauth, V. Caignaert, I. Mirebeau, G. Baldinozzi, Phis. Rev. B 61 (2000) 871–874.
[20] R.D. Shannon, Acta Crystallogr. A 32 (1976) 751–767.
[21] J.E. Huheey, Inorganic Chemistry, Harper & Row, New York, 1983.
[22] V. Cherepanov, T. Aksenova, E. Kiselev, L. Gavrilova, Solid State Sci. 10 (2008) 438–443.
[23] M. Katsuki, S. Wang, M. Dokiya, T. Hashimoto, Solid State Ionics 156 (2003) 453–461.